Near Surface Geophysics | EAGE EUROPEAN ASSOCIATION OF GEOSCIENTISTS & ENGINEERS

ORIGINAL ARTICLE

Resistivity imaging of river embankments: 3D effects due to varying water levels in tidal rivers

John Ball[1,2] | **Jonathan Chambers[2]** | **Paul Wilkinson[2]** | **Andrew Binley[1]**

[1]Lancaster Environment Centre, Lancaster University, Bailrigg, Lancaster, UK

[2]British Geological Survey, Keyworth, UK

Correspondence
John Ball, Lancaster Environment Centre, Lancaster University, Bailrigg, Lancaster, LA1 4YQ, UK.
Email: j.ball4@lancaster.ac.uk

Abstract

Electrical resistivity tomography (ERT) has seen increased use in the monitoring the condition of river embankments, due to its spatial subsurface coverage, sensitivity to changes in internal states, such as moisture content, and ability to identify seepage and other erosional process with time-lapse ERT. Two-dimensional ERT surveys are commonly used due to time and site constraints, but they are often sensitive to features of anomalous resistivity proximal to the survey line, which can distort the resultant inversion as a three-dimensional (3D) effect. In a tidal embankment, these 3D effects may result from changing water levels and river water salinities. ERT monitoring data at Hadleigh Marsh, UK, showed potential evidence of 3D effects from local water bodies. Synthetic modelling was used to quantify potential 3D effects on tidal embankments. The modelling shows that a 3D effect in a tidal environment occurs (for the geometries studied) when surveys are undertaken at high water levels and at distances less than 4.5 m from the electrode array with 1 m spacing. The 3D effect in the modelling is enhanced in brackish waters, which are common in tidal environments, and with larger electrode spacing. Different geologies, river water compositions, and proximities to the model parameters are expected to induce a varied 3D effect on the ERT data in terms of magnitude, and these should be considered when surveying to minimize artefacts in the data. This research highlights the importance of appropriate geoelectrical measurement design for tidal embankment characterization, particularly with proximal and saline water bodies.

KEYWORDS
electrical resistivity tomography, embankment, modelling, site effect

INTRODUCTION

Flood embankments are essential defence infrastructure for protecting sites of societal and economic importance. Such structures can suffer deterioration through time because of internal erosion processes (e.g., piping and suffusion) (Almog et al., 2011; Bersan et al., 2018; Planès et al., 2016; Wang et al., 2018; Yang & Wang, 2018), external erosion (e.g., animal burrowing and scouring by rivers) (Borgatti et al., 2017; Dunbar et al., 2017; Jones et al., 2014) and slope failure

(Dunbar et al., 2017). Therefore, regular monitoring of flood embankments is vital to identify degradation, which may lead to failure of its serviceability limit state through, for example, seepage or slumping.

Traditionally, monitoring of flood embankments involves walkover surveying and geotechnical investigations. Walkover surveys are limited by an inability to detect internal problems where there is no expression of embankment degradation (e.g., soil swelling) at the surface and obscuration by vegetation (Jones et al., 2014; Sentenac et al., 2018). Geotechnical investigations can

provide reliable and relevant data for assessment of the internal conditions of the embankment, but are limited by low spatial and volumetric coverage (Michalis et al., 2016), where extensive investigation is difficult due to their invasive and destructive nature, and the parameters obtained from such investigations are only reliable for the location of the sampling point (Cardarelli et al., 2014).

Geophysical techniques have been increasingly utilized because they are non-invasive (Michalis et al., 2016), are sensitive to changes in the sub-surface which may indicate structural degradation (Jones et al., 2014; Moore et al., 2011) and have the potential to infer geotechnical properties through appropriate petrophysical relationships, as obtained from intrusive investigations and subsequent geotechnical monitoring (Chambers et al., 2014; Gunn et al., 2018; Zhang & Revil, 2015). One commonly used geophysical technique for monitoring flood embankments is electrical resistivity tomography (ERT) (e.g., Amabile et al., 2020, Bièvre et al., 2018; Camarero et al., 2019; Fargier et al., 2014; Jodry et al., 2019; Jones et al., 2014; Michalis & Sentenac, 2021; Rittgers et al., 2015; Tresoldi et al., 2018) due to its sensitivity to porosity, clay content, pore water conductivity (Binley & Slater, 2020), moisture content (Fargier et al., 2014) and internal structure (Chambers et al., 2014), making it useful for detecting subsurface changes which may indicate embankment degradation.

Despite the greater spatial coverage possible with ERT compared to standard geotechnical sampling, and ability to image sub-surface conditions, uncertainties in interpretation of data still exist. One such problem is the 3D effect, in which proximal, but off-survey, resistivity distributions can influence the resistivity values directly beneath the ERT line; Fargier et al., 2014; Hung et al., 2019; Nimmer et al., 2008) under a 2.5D assumption. These can arise from factors such as topographic effects, heterogeneous geology and features of anomalous resistivity nearby, such as a buried pipeline. In a river embankment setting, a key source of a three-dimensional (3D) effect is likely to be the river. Furthermore, a river of a variable stage (water level) and/or fluid electrical conductivity (e.g., from tidal influence) may lead to temporally variability of such 3D effects. Further references to a 3D effect on the data will be related to river-induced effects unless otherwise stated.

On embankments, ERT data are commonly acquired using linear (two-dimensional "2D") electrode arrays, because of the relatively fast inversions and fieldwork convenience, where ERT surveys on an embankment are typically set up on the crest, parallel to the river bank. The 2.5D inversion method (following references to 2D inversion imply the 2.5D assumption) assumes that the resistivity does not vary in the direction perpendicular to the vertical plane below the line. The perpendicular topographic variations of the embankment and chang-

ing water levels to the side violate this assumption (Cho et al., 2014). As such, the data acquired from a 2D survey may be influenced by features adjacent to the survey, for example. lower resistivities from an adjacent river may be mapped onto a 2D survey along a dam crest creating artefacts that are not present in reality.

Normalization methods and combined models have been used to remove influence of some 3D effects which apply to all ERT surveys, such as topography (e.g., Bièvre et al., 2018; Fargier et al., 2014). Other authors have looked at specific 3D effects which might impact ERT data. For example, Hung et al. (2019) investigated the impact on ERT data of a pipe buried proximal to a 2D electrode array. They examined the effects of resistivity ratios between pipeline resistivity and the modelled geology resistivity, pipeline size, embedded depth, electrode spacing, and distance from the source of the 3D effect to the electrode array. Through this, they identified that resistivity ratios of less than 0.1 and large pipeline sizes induce greater 3D effects; pipeline emplacement at greater depths will induce weaker 3D effects, and electrode spacing variations had minimal change in the magnitude of 3D effect observed. This suggests that an adjacent river will induce a significant 3D effect on an ERT survey, given its larger size than a pipeline.

Laboratory (scaled physical model) experimentation has also been used by Hojat et al. (2020) to explore the 3D effect induced by rivers. Their experiment involved filling a plexiglass tank, containing a scaled model of a river levee, with water. Surveys were undertaken at various water levels to represent seasonal variations in water level, and a significant 3D effect was induced by the water body. Through this, they observed changes in apparent resistivity to true resistivity ratios with different electrode spacings. Through laboratory experimentation, it was shown that the 3D effect is larger with increased electrode spacings, because of greater depths of investigation inducing larger sensitivities at depth and hence greater coverage that is potentially affected by adjacent resistivities (Hojat et al., 2020). Further synthetic modelling showed that 3D effects have the potential to decrease with a further increase of electrode spacing, as a decrease in shallow resolution will result in the source of the 3D effect having smaller impact on neighbouring data (Hojat et al., 2020) when the source has a fixed position. The 3D effect varies with seasonality, where peak distortions in resistivity in the ERT array are present within winter, predominantly at greater depths below the surface (Tresoldi et al., 2019).

This study aims to build upon these previous approaches to investigate the effect of a tidal influence of a river on ERT data obtained from surveys on the embankment crest. Synthetic models simulating varying water levels and salinities, for a homogeneous and heterogeneous embankment, are used to investigate the relationship between measurement and survey design and 3D artefacts, for the purpose of identifying improved

ERT deployment approaches for tidal embankment monitoring. Previous research has produced contrasting conclusions regarding the relationship between electrode spacing and the magnitude of the 3D effect (e.g., Hojat et al., 2020; Hung et al., 2019). Therefore, further synthetic modelling will be used to help confirm the effect of electrode spacing on the magnitude of 3D effect present from a river proximal to an ERT array.

Alongside synthetic modelling, time-lapse ERT monitoring from the Hadleigh Marsh field site on the Thames estuary, United Kingdom, is used to illustrate potential 3D effects in ERT applied to flood defence monitoring. The series of modelling experiments applied to a synthetic river embankment is performed to examine resistivity features representing a watercourse adjacent to a survey line impact on ERT data. We then offer recommendations on approaches to mitigate a 3D effect, including survey design recommendations and application of methodologies during inversion.

SYNTHETIC MODELLING

Methodology

To quantitatively assess the impact of the 3D effects resulting from tidal variations on 2D ERT data parallel to a watercourse, in terms of river water level and resistivity, two synthetic modelling scenarios were designed to simulate a river retreating with a waning tide. In both models, an electrode array, consisting of 48 electrodes at 1 m spacing, was located along the embankment, parallel to the watercourse (see, Figure 1). The embankment crest is 3 m wide, and the array is situated at the midpoint of the crest width. The riverside slope angle is 14°, and the river has a maximum width of 27.8 m. In the associated finite element mesh, the modelled river extended for 101 m beyond the first and last electrode in the orientation parallel to the array. This ensured that the river was sufficiently long to reduce boundary effects or influences on the data from resistivity contrasts between the end of the river in the mesh and the background region. Topography was included in the inversion in order to account for its influence on the ERT data. Scenario one involved a homogeneous embankment, while scenario two included a clay core of differing resistivity to explore the impact of such heterogeneity. The embankment geometry is shown in Figure 1.

Utilizing the mesh generation software Gmsh (Geuzaine & Remacle, 2020), a 3D unstructured finite element mesh was generated, allowing creation of regions representing the river, embankment and clay core for scenario two, each of which can be assigned specific resistivity values. Once the mesh was generated and resistivities were assigned to the river, embankment and clay core, the ERT code R3t (Binley & Slater, 2020) was used to compute a forward model

for a specific scenario. R3t was used, instead of 2D modelling software, due to the ability of a 3D modelling set-up to incorporate external features into the model. Once the forward model was complete, 2% random (Gaussian) noise was added to the resultant apparent resistivities. Following this, the data were inverted in 3D, in order to simulate an inversion of ERT data with an adjacent river which could potentially induce anomalous artefacts in the inversion. The inversions for all models incorporated the 3D geometry of the embankment, enabling topography to be accounted for, reducing the 3D effect associated with this. Each inversion utilized smoothness-constrained (i.e., L_2 norm) regularization.

Wenner, Schlumberger, and dipole–dipole array configurations were modelled in order to determine the likely impact of a 3D effect based on array configuration. For this, using a river level of 2.95 m at a 1.7-m distance from the electrodes, models were run with electrode sequences corresponding to each configuration and synthetic measurements could then be compared. From this, the electrode configuration with the most severe 3D effect was selected for subsequent modelling. For all electrode configurations, an a spacing of 1–4 m was selected. The Schlumberger array had an n of 1–9, and the dipole–dipole configuration had an n of 1–9.

In order to study the effect of changes in river level, the finite element mesh was adjusted for a given river level; the modelled river was decreased by 5 cm vertically, and the riverfront was retreated 20 cm laterally per model scenario (see Figure 1b), which represented a waning tide. The initial conditions were a river that was 1.7 m from the electrode array, at a river height 5 cm lower than the crest elevation (see Figure 1). For each river level, four separate forward models and inversions were undertaken, where river resistivities were assigned as 1, 5, 10 and 20 Ωm for each scenario, in order to account for varied river salinities. Once the inversions for each modelled river salinity were completed for the given river level, the synthetic river level was decreased and models were run as before. From this, resistivity values underlying the electrode array could be obtained, allowing comparison between models as to the magnitude of the 3D effect with changing water levels and river salinities. The process described was repeated for every reduction in river level until there was no observed change in resistivity underlying the ERT array from a 3D effect after inversion for all modelled river resistivities.

The homogeneous river embankment was assumed to consist of a clay fill, representing a common construction material for embankments. The assumed resistivity of the embankment was taken to be 40 Ωm, based on typical resistivity values for clay (Palacky, 1987). The second modelling scenario consisted of a more conductive clay core, set at 10 Ωm, with a more resistive 40 Ωm infill, to test for effects of heterogeneity in a set-up representative for such embankments The water in estuarine environments is typically brackish (Sandrin et al., 2009),
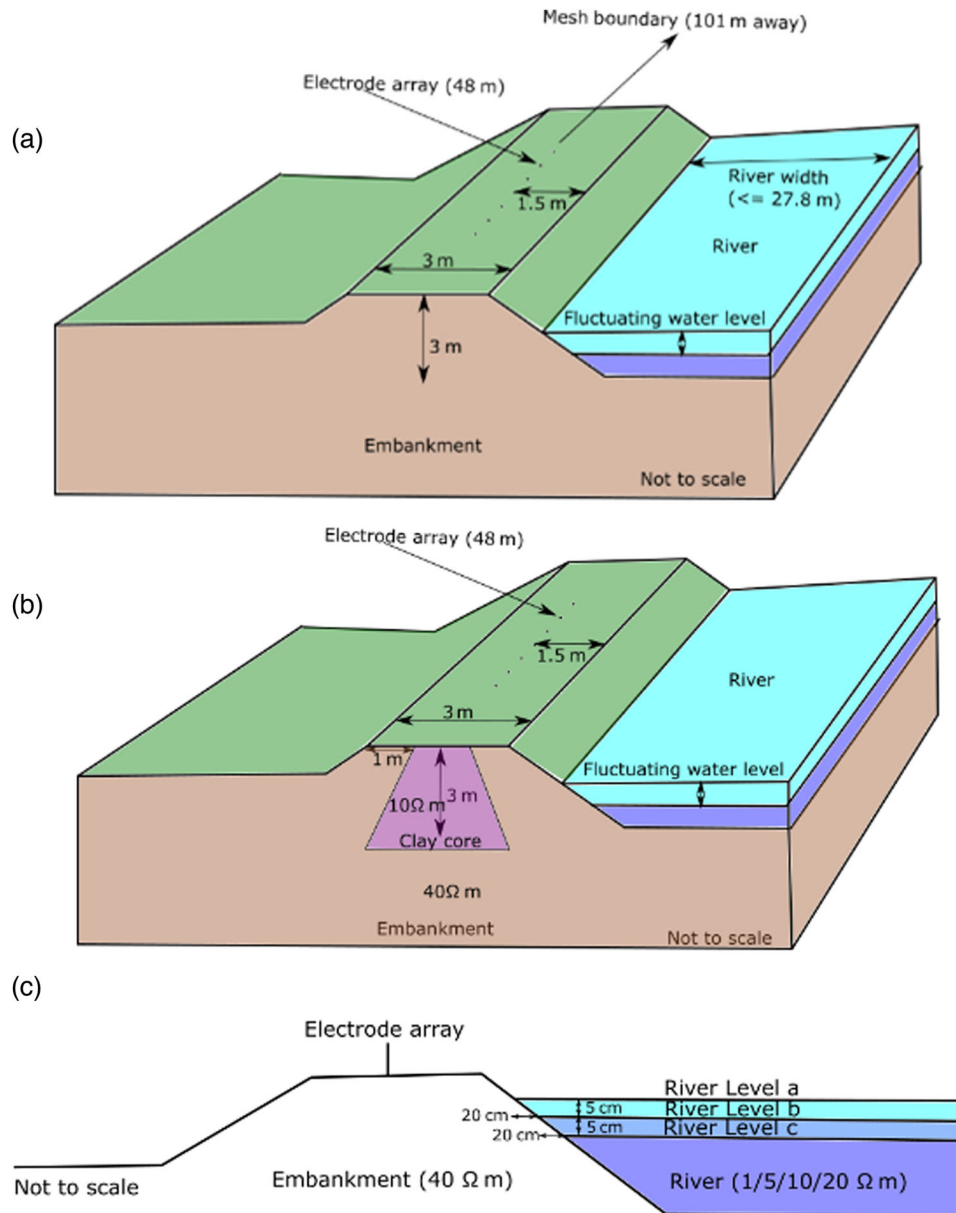
FIGURE 1 Geometrical representations of the synthetic model problem. (a) The layout of the embankment, river and electrode array orientation for the homogeneous model. The electrode array is located parallel to the river and is situated at the centre of the embankment crest. (b) The heterogeneous model, including the clay core. (c) A 2D cross-sectional image of the synthetic embankment, showing the adjustments to river geometries with each iterant model and modelled river resistivities, representing salinity changes.

so models included ranges of resistivities typical of more brackish water and freshwater, 1, 5, 10, and 20 Ωm, the latter representing freshwater rivers with some tidal influence (Palacky, 1987). In addition, modelling procedures were repeated for different electrode spacings to observe the effect of spacing on the associated 3D effect from a tidal setting.

Synthetic modelling results

The synthetic models were developed and analysed to explore three variables: the effect of a change in dis-tance between the river and the electrode array; the change in river electrical conductivity (representing a change in salinity); and the electrode spacing used for the survey. Through this, the nature and severity of the 3D effect resulting from changes in salinity and water level can be understood and therefore methods to mit-igate the impact can be made. In embankments with greater crest heights, a larger electrode spacing may be chosen to achieve greater depth penetration. Therefore, greater electrode spacings have been modelled to deter-mine potential impacts of a 3D effect where a different electrode setup may be selected for this survey scenario.
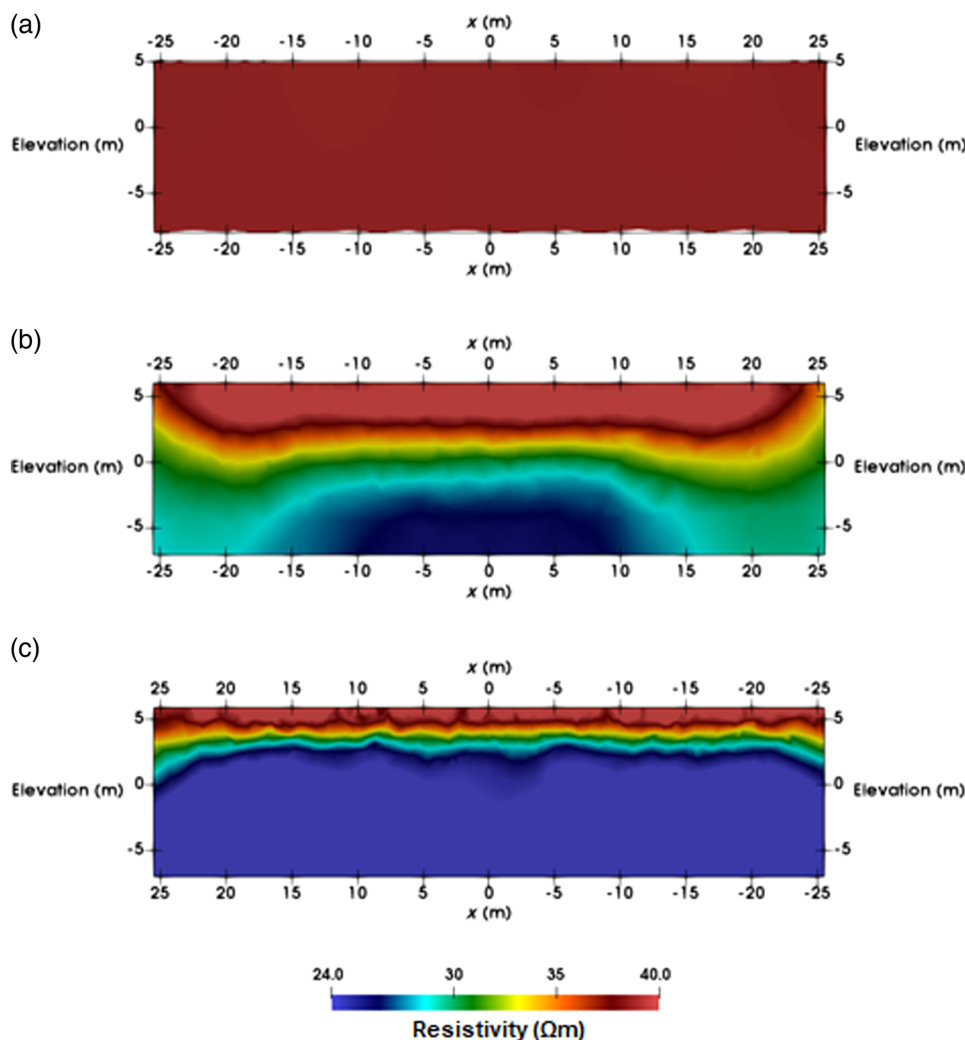
FIGURE 2   Inversions, showing the 3D effect resulting from differing array types, where the inverse image represents the synthetic subsurface resistivity distribution directly beneath the electrode array. (a) Wenner configuration. (b) Schlumberger configuration. (c) Dipole–dipole configuration. For each configuration the river is 1.7 m from the embankment, the river is 0.5 m below crest height, and the river resistivity is 1 Ωm. The resistivity of the embankment is 40 Ωm. In each image, the embankment height is 5 m.

Array configurations

The results for the synthetic modelling of Wenner, Schlumberger, and dipole–dipole arrays, using the homogeneous embankment model, are shown in Figure 2. For comparison, the maximal river level was selected, using 1 Ωm as a river resistivity, in order to demonstrate the maximum possible impact of a 3D effect from each array type.

As shown in Figure 2, the resistivities for the dipole–dipole array (Figure 2c) are more affected by a 3D effect than the other array configurations, suggesting a greater lateral (off-plane) sensitivity for this array. For the Wenner array (Figure 2a), with a spacing of 1 m, there is unlikely to be any significant 3D effect, but it may be more of an issue if greater electrode spacings are selected for a survey. The Schlumberger array (Figure 2b) shows influence from a 3D effect induced by the river, but with poorer model resolution compared with dipole–dipole. Therefore, for the purpose of the further synthetic modelling a dipole–dipole array has been selected because of the greater apparent sensitivity to off-plane effects.

Distance of river from the electrode array

Selected inversions taken from the different modelled river levels were chosen for assessing the resistivities directly underlying the ERT survey for both modelling scenarios. For each model in the homogeneous embankment scenario, the embankment resistivity is 40 Ωm, so a significant deviation from this, which gives greater distortion than what can be expected from noise alone, is inferred to be a 3D effect, induced by the modelled river. Likewise, for the heterogeneous model, the clay core resistivity is 10 Ωm, with a 40-Ωm background
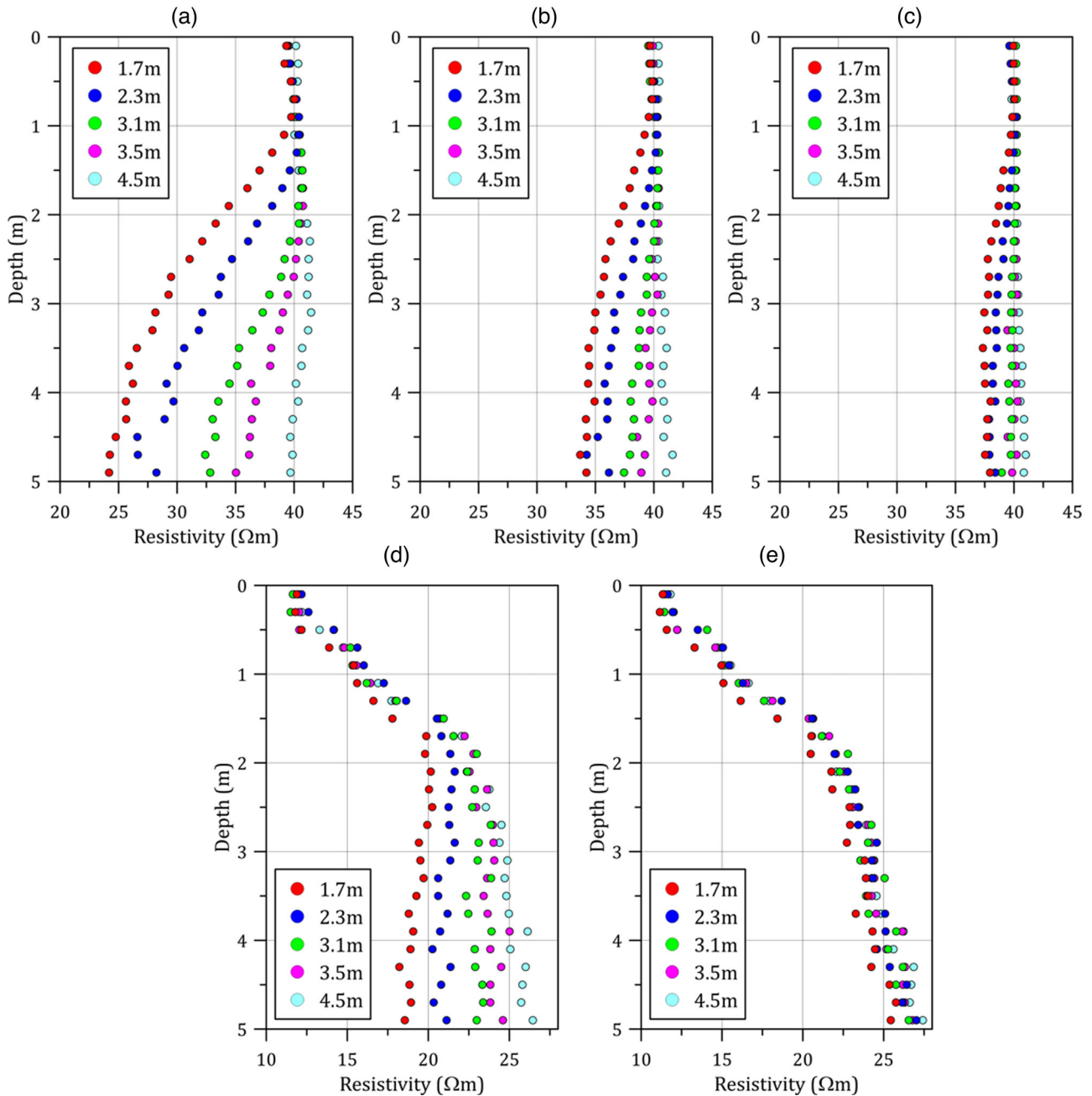
FIGURE 3 Profiles of resistivity variation below the synthetic ERT array for different river levels in different modelled river resistivities (a) where the river is 1 Ωm and the model is homogeneous. (b) 5 Ωm and the model is homogeneous. (c) 10 Ωm and the model is homogeneous. (d) 1 Ωm and the model is heterogeneous. (e) 10 Ωm and the model is heterogeneous. The models associated with a river of 20 Ωm are not shown, due to the lack of distorted resistivities underlying the electrode array for all distances from the river to the electrode.

resistivity for the remainder of the subsurface, meaning deviations from this represent influence from a 3D effect. Figure 3 is a representation of the resistivities at various depths beneath the ERT array for the synthetic models, showing the resistivities for each modelled water level.

From the models, as is evident in Figure 3, there is a distinct effect on resistivities located at greater depths below the ERT line, while at depths less than 1 m the effect is negligible. As expected, the effect is more severe

where the river is closer to the electrode array, with less pronounced distortions to resistivity with decreasing river level. For the most proximal river level in the homogeneous model, resistivities can reduce by approximately 15 Ωm at depths of 3.5 m below the array when the river is least resistive. The magnitude of the effect reduces until the river reaches 4.5 m from the electrode array, where the resistivities approximate to 40 Ωm for every modelled river resistivity (i.e., there is no 3D
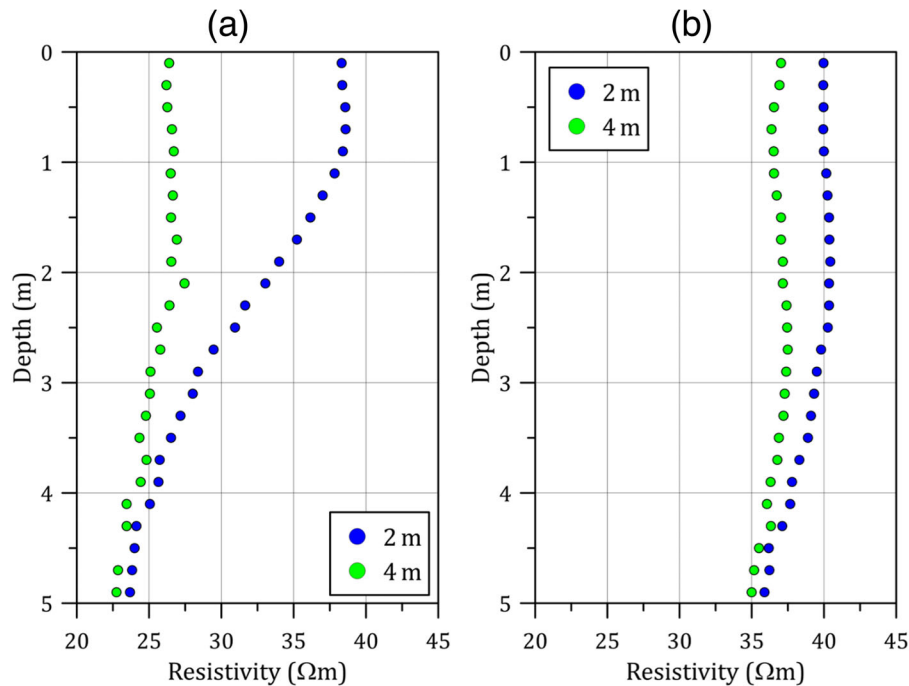
FIGURE 4 Resistivities directly underneath the modelled ERT array across the embankment crest, showing resistivity across depth below the surface, for different electrode spacings. (a) When the river is 1.7 m from the electrode array. (b) When the river is 3.5 m from the electrode array.

effect). Slight discrepancies in the trend with depth are likely impacts of adding 2% noise to the apparent resistivities prior to inversion. The noise does not obscure the trend in the models, indicating that anomalous resistivities from the inversion can be ascribed to the 3D effect induced by changing river levels or salinities, as opposed to random background effects, in a real-life scenario where noise will be present.

In the heterogeneous models (Figures 3d and 4e), with decreasing river level there is no obvious associated trend in resistivity at shallow depths, indicating that resistivity variation is driven by influences from the embankment and 2% added Gaussian noise, not effects from the river at approximately 0.0–1.5 m depth. This is in contrast to depths below 1.5 m, where the resistivities are noticeably less resistive with higher river levels, more proximal to the electrode array. As with the homogeneous model, this indicates that the 3D effect from the river is more pronounced with depth, using a 1-m electrode spacing, and embankment heterogeneity does not obscure such a trend in 3D effect.

River salinity

The plots in Figure 3 also show a distinct reduction in resistivity with increased modelled river salinities for both a homogeneous and heterogeneous embankment. It is evident from Figure 3 that the trend of the resistivities for modelled river levels is less steep with increased

river resistivity. The effect is most pronounced for the modelled river salinity of 1 Ωm, with a clear decrease in resistivity at depth when the river is proximal to the electrode array. When the modelled river is 20 Ωm, negligible 3D effects are seen. This indicates that a significant 3D effect in river embankments will be most prominent in estuarine environments where water is likely to be brackish. With higher modelled resistivities for the river, which represent freshwater environments, the associated 3D effect is negligible across all river levels. In conditions like this, freshwater is unlikely to induce an impact (provided the array is far enough away from the water body) and a 3D effect would be limited to estuarine or coastal environments.

As a decrease in salinity also reduces the magnitude of the 3D effect in the heterogeneous scenario at depths shallower than the base of the modelled core, it indicates that the bulk of the induced 3D effect, at shallow depth, arises from changes in river level and associated resistivity. However, for all models the resistivity does not trend towards the modelled value of 40 Ωm. This is likely a result of the embankment heterogeneity and modelled clay core values above influencing resistivity values at greater depth.

Electrode spacing

Plots of resistivities underneath the ERT array for different electrode spacings are shown in Figure 4. The river resistivity is set at 1 Ωm, and selected distances

of electrode array from the river (1.7 m and 3.5 m) are shown for comparison. The plots show the effect of electrode spacing of the electrode array, utilizing the same mesh characteristics. It is evident that with increased electrode spacing there is an associated decrease in resistivity at the ERT array. For an electrode spacing of 4 m, marked decreases of resistivity to 25 Ωm are present at shallow depths when the river is most proximal, whereas this is not the case for electrode spacings of 2 m. The results from electrode spacings of 1 m are not shown in the figure, because resistivities are marginally higher, and similar in trend to 2 m spacing. This indicates that for large surveys with very large electrode spacings there will be a significant 3D effect at the ERT array at all depths, which would obscure any underlying features which may be present underneath the embankment when the river level is most proximal to the electrode array. This suggests that for smaller electrode spacings the higher resolution and the shorter influence distances from the river help reduce the 3D effect, especially at shallow depths.

Embankment heterogeneity

Resistivities for the modelling of the more heterogeneous embankment, consisting of clay core, are represented in Figure 3d,e. Resistivity values proximal to the surface, in the region of the 10-Ωm clay core, varied between 11 Ωm and 13 Ωm. This indicates that the 40-Ωm infill modelled for the rest of the embankment has a weak influence on resistivities at shallow depth. Therefore, embankment heterogeneity and complexity are potential sources of a 3D effect, which may influence interpretation of data.

Resistivities at depth, below the clay core, do not trend towards the set value of 40 Ωm, levelling out at 25–30 Ωm. This is likely due to embankment heterogeneity and weak measurement sensitivity at depth: resistivities in the region below the clay core are influenced by the resistivity assigned to the core.

Overall, trends in resistivity between the homogeneous and heterogeneous models are similar, with decreasing resistivities at depth with declining river levels and salinities.

Sensitivity distribution

As outlined in Binley and Slater (2020), there are a number of image appraisal methods available for assessing an inverse model. The computational demands of calculating a model resolution matrix are often prohibitive for 3D problems, and so a cumulative sensitivity approach (see, Binley & Slater, 2020) is adopted here. Figure 5 shows a cumulative sensitivity distribution (produced by R3t) for the synthetic modelling, using 1 m electrode

spacing, for when the river level is at its lowest. It can be seen from this that there is measurement sensitivity within the region of the river, indicating that a 3D effect can be detected by the array for this and all other scenarios, where the river will be more proximal to the array.

HADLEIGH MARSH

The Hadleigh Marsh embankment is approximately 4 km long and 65 m wide (Essex County Council, n.d.). The embankment serves as a flood defence on the northern margin of the Thames estuary and is situated on an eroding coastline (Brand & Spencer, 2019). The present embankment consists of a historic clay embankment, which was subsequently raised in the 1980s using household and commercial landfill waste, capped with puddled clay (Brand & Spencer, 2019). Historical maps suggest that an embankment has existed since the 19th century. Current embankment construction predates required legislation for records of such embankments to be kept, so comprehensive details of waste composition are unknown (Secretary of State, 2002). Hadleigh Marsh is situated in an SSSI (site of special scientific interest), it is a marine-protected area (Brand & Spencer, 2019) and is within the bathing water zone of influence catchments for eight public beaches along the Thames (Environment Agency, 2017). Therefore, it is imperative that the integrity of the embankment is maintained to a suitable standard, so that waste material and leachates do not contaminate the local environment.

Geophysical characterization was undertaken at Hadleigh Marsh to reveal embankment structure and moisture-driven processes within the asset that could be related to tidal forcing, contaminant transport and slope stability. To facilitate long-term monitoring, an automated ERT measurement system, referred to here as PRIME (Holmes et al., 2020), was installed at the site. The system enables near-real-time ERT data collection and has been powered by batteries charged by a solar panel, with remote operation and data retrieval achieved through a 4G telemetric link. The system was attached to five linear electrode arrays, with two orientated approximately parallel to the estuary front and three perpendicular (Figure 6). ERT surveys on all electrode arrays were generally acquired once every 3 days for each line from the April 2017 to present. The electrodes spacings were 2 m, utilizing dipole–dipole measurement configurations with a spacings of 2–46 m and n in the range of 1–7, where an a spacing is the current and potential dipole sizes and n is the current and potential dipole separation.

Time-lapse ERT data from the site were inverted to visualize changes in resistivity with differences in tides, using ResIPy (Blanchy et al., 2020). Initial inversions focused on 2D inversions of line L2 (Figure 6), which was
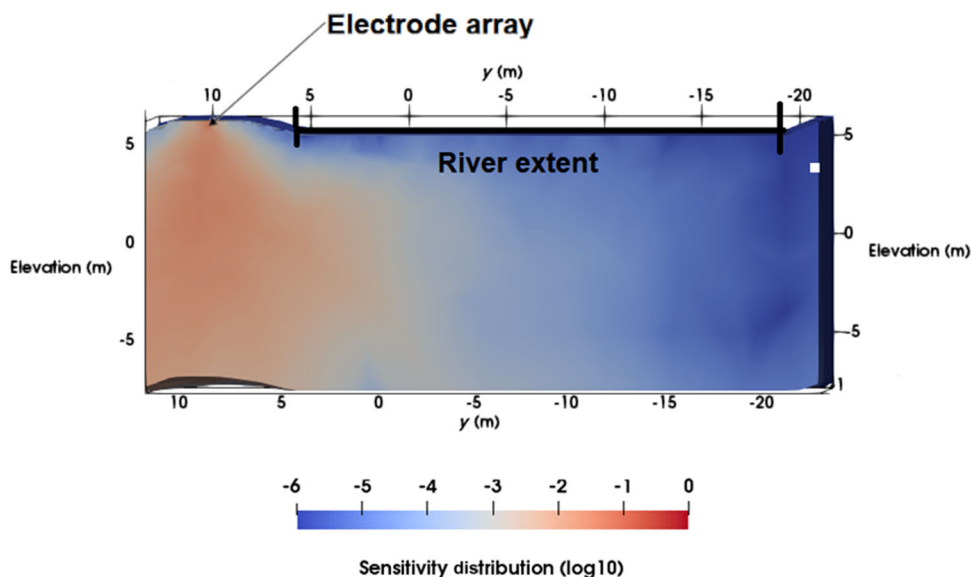
FIGURE 5   Cumulative sensitivity distribution for the synthetic model outputted from R3t, including an outline of the river region and electrode array for where the river is at its furthest. This sensitivity map is cropped half-way across the mesh, in the direction perpendicular to the embankment, to show how sensitivity is distributed. The electrode array is located at 9.5 m in the *y* orientation.

FIGURE 6   Layout of the PRIME array at Hadleigh Marsh, where L1 and L2 are ERT lines parallel to the riverfront and P1–P3 are ERT lines perpendicular.

the closest line to the estuary and for which the greatest 3D effect due to tidal influence was expected. As with the synthetic model, it is approximately parallel to the river course but is not located on the embankment crest. The 2D time-lapse inversions were undertaken using the difference inversion method (LaBrecque & Yang, 2001). A 3D inversion was also undertaken, incorporating all ERT lines as a means of addressing whether anomalies present in line L2 from a 2D inversion were a result of 3D effects on 2D data. Tidal information taken from the

nearby Sheerness tidal gauge (obtained from the British Oceanographic Data Centre) provided the tidal ranges across the year and was used for selection of data for time-lapse analysis based on the tidal cycle. For each time-lapse inversion, a period of low tide, corresponding with survey timings, was selected for the reference model and the time-lapse inversion continued until the next high tide occurred during the survey period. Several tidal cycles were selected for separate time-lapse inversions, taken at different points in the year, in order
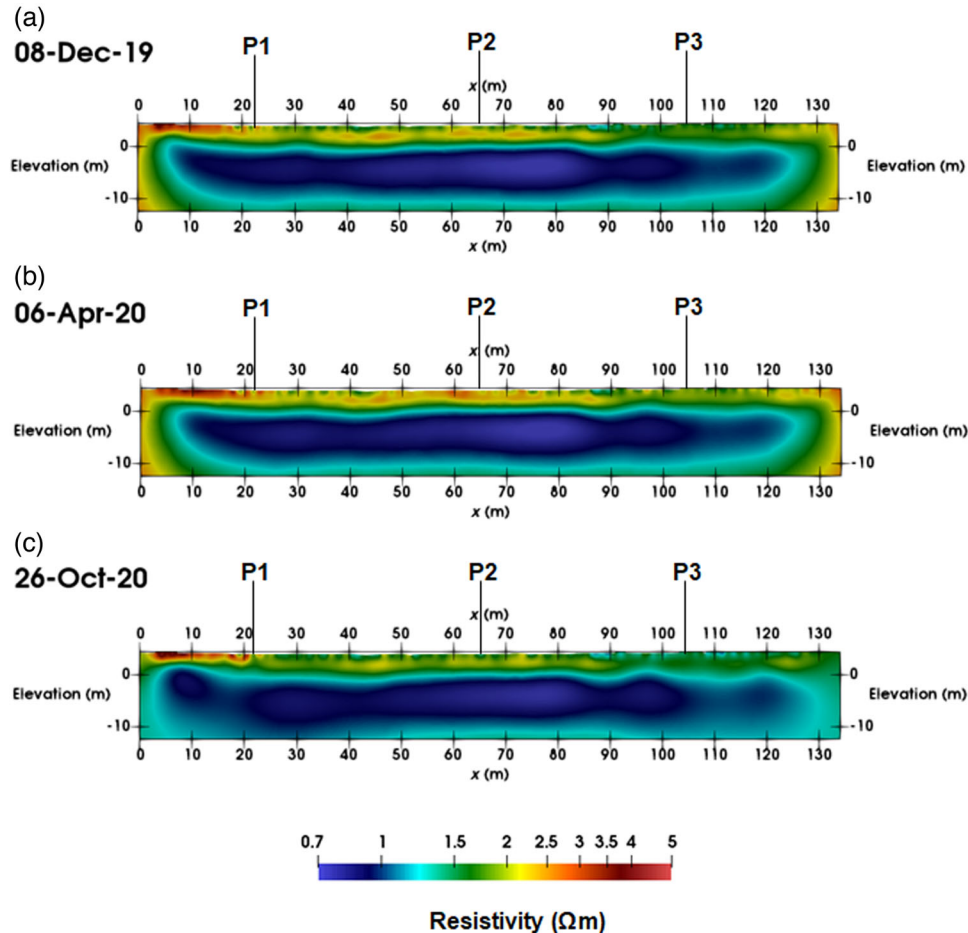
FIGURE 7 2D inversions of the ERT data taken from L2 at Hadleigh Marsh (see Figure 2) where each inversion represents the start of a tidal cycle, where it is at a tidal minimum. (a) A reference inversion from 08-Dec-19 (water level 1.08 m). (b) 03-Apr-20 (water level: 1.65 m). (c) 26-Oct-20 (water level: 1.35 m). Water levels were taken from Sheerness tidal gauge, so water levels are an analogous correspondence to Hadleigh Marsh.

to help assess the seasonal impact. For each time-lapse inversion, the reference model was selected as that corresponding to a tidal minimum; data from subsequent dates in that tidal cycle were included for the inversion (the last dataset corresponding to the point prior to the next tidal minimum).

Hadleigh Marsh results

To explore the potential 3D effect of the River Thames on 2D ERT data at Hadleigh Marsh, 2D inversions were undertaken on the most proximal line to the river, L2, and the intersecting orthogonal lines, P1-P3 (Figure 6). Representative inversions of L2 are shown in Figure 7, taken from the start of a waxing tidal cycle for their respective time cycle and as such represent the initial tidal minimum. In order to demonstrate the tidal nature of any associated 3D effects, a subsequent time-lapse inversion was undertaken when tides were increasing, where the data from Figure 7 were used as a reference dataset, and any changes have been related to

these tidal variations. Figure 8 shows the results of the time-lapse inversion.

The reference inversions for all data sets shown in Figure 7 indicate a conductive subsurface adjacent to the river, where resistivity values are typically less than 10 Ωm. However, the upper 2 m is slightly more resistive than at greater depths. It is possible that this is a feature of this section of the embankment, or an effect of prior weather conditions, where greater depths are likely to be more saturated and therefore less resistive. However, a 3D effect resulting from a river is likely to induce a conductive feature at depth, as evident in the synthetic modelling, where decreased resistivities are present at depths below 2 m from the surface. This may explain the trends observed, creating difficulties in the reliability of interpretation. In order to observe changes due to a 3D effect induced by tide, time-lapse inversions have been shown at different points in the tidal cycle, where water level was higher than in the reference inversion.

The difference inversions for L2 show generally small changes in resistivity from the start of the tidal cycle to a time of high-water level. In most inversions, a decrease
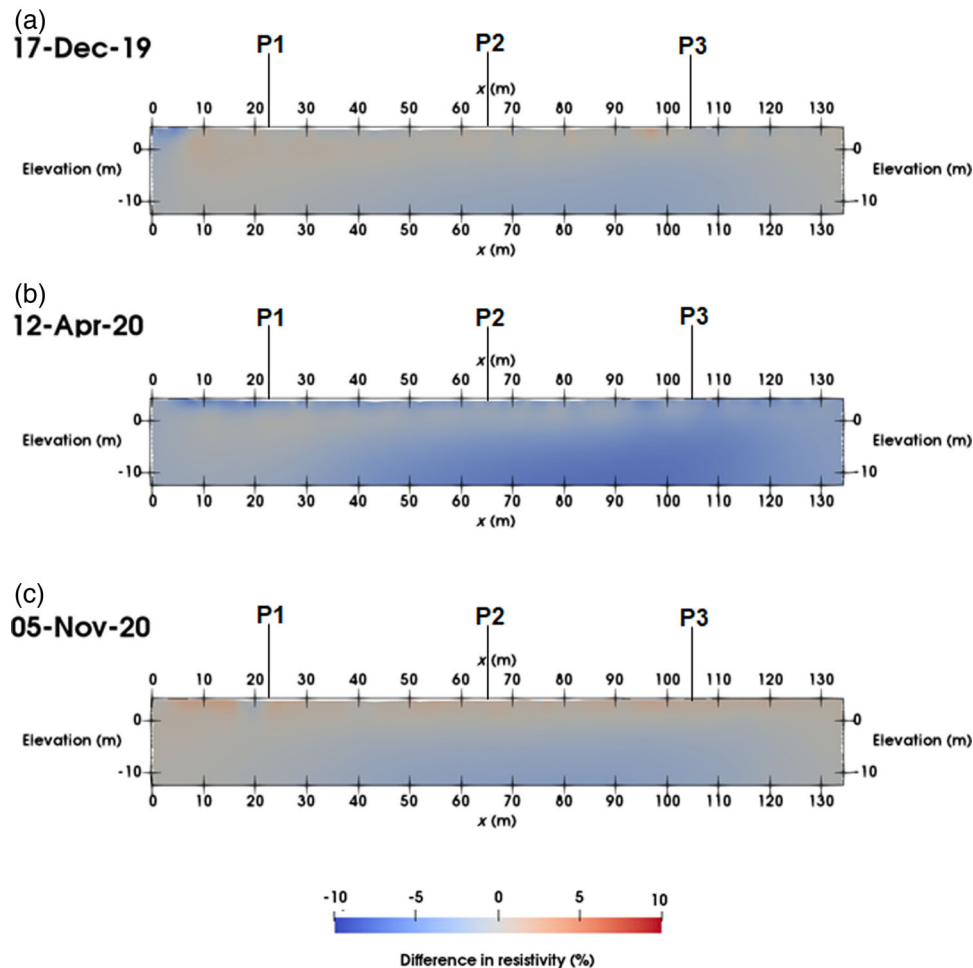
FIGURE 8 2D difference inversions for L2 at Hadleigh Marsh. Each difference inversion shown corresponds to the reference inversion of the same letter shown in Figure 7. (a) 17-Dec-19 (water level: 5.64 m, reference inversion: 03-Dec-19). (b) 12-Apr-20 (water level: 5.75 m, reference inversion: 03-Apr-20). (c) 05-Nov-20 (water level: 5.47 m, reference inversion: 26-Oct-20). Water levels were taken from Sheerness tidal gauge, so water levels are an analogous correspondence to Hadleigh Marsh.

in resistivity of greater than 5% is noted from depths lower than 5 m for approximately 80 m across the embankment to the left of the section. This is potentially an effect induced by the proximal river, where higher tides are inducing a stronger 3D effect at depths where potential 3D effects are noted in the reference inversions. This part of the section is most proximal to the river (Figure 6), which gives weight to this interpretation. However, due to the low magnitudes, other lateral effects or over/underfitting of data cannot be ruled out. At shallow depths, resistivity variation is not significantly affected by tidal action. Overall, the data show some potential impact at depths, which may correspond to a 3D effect from the river. The April 2020 dataset shows the greatest decrease in resistivity through time, likely due to the ground being less saturated, meaning resistivity contrasts between river and ground beneath the electrode array will be larger.

The 2D inversions of P1-P3 (Figure 9) are generally more resistive than L2, which is assumed to be a result

of the landfill infill, with less resistive anomalies close to the river Thames. Subsequent time-lapse inversions of P1-P3 (Figure 10) show an overall increase in conductivity, assumed to be a result of infiltration from rainfall due to the presence of rainfall in the days following the December reference inversion.

Data from all five electrode lines (see, Figure 6) were utilized in a 3D time-lapse inversion for each tidal cycle at Hadleigh Marsh. Several inversions were run for various tidal cycles across the PRIME monitoring period at Hadleigh Marsh (08-Dec-19 to 17-Dec-19); Figure 11 shows a fence diagram of a selected reference inversion for the ERT, at low tide.

The 3D inversion shows a general consistency in resistivity across each ERT line for the December 2019 dataset. The perpendicular lines, P1–P3, are generally resistive, with similar magnitudes to their 2D inversion counterparts (see Figure 9). Whereas, L1 and L2 are less resistive than P1-P3, which is believed to be influence from the Thames adjacent to L2 and the
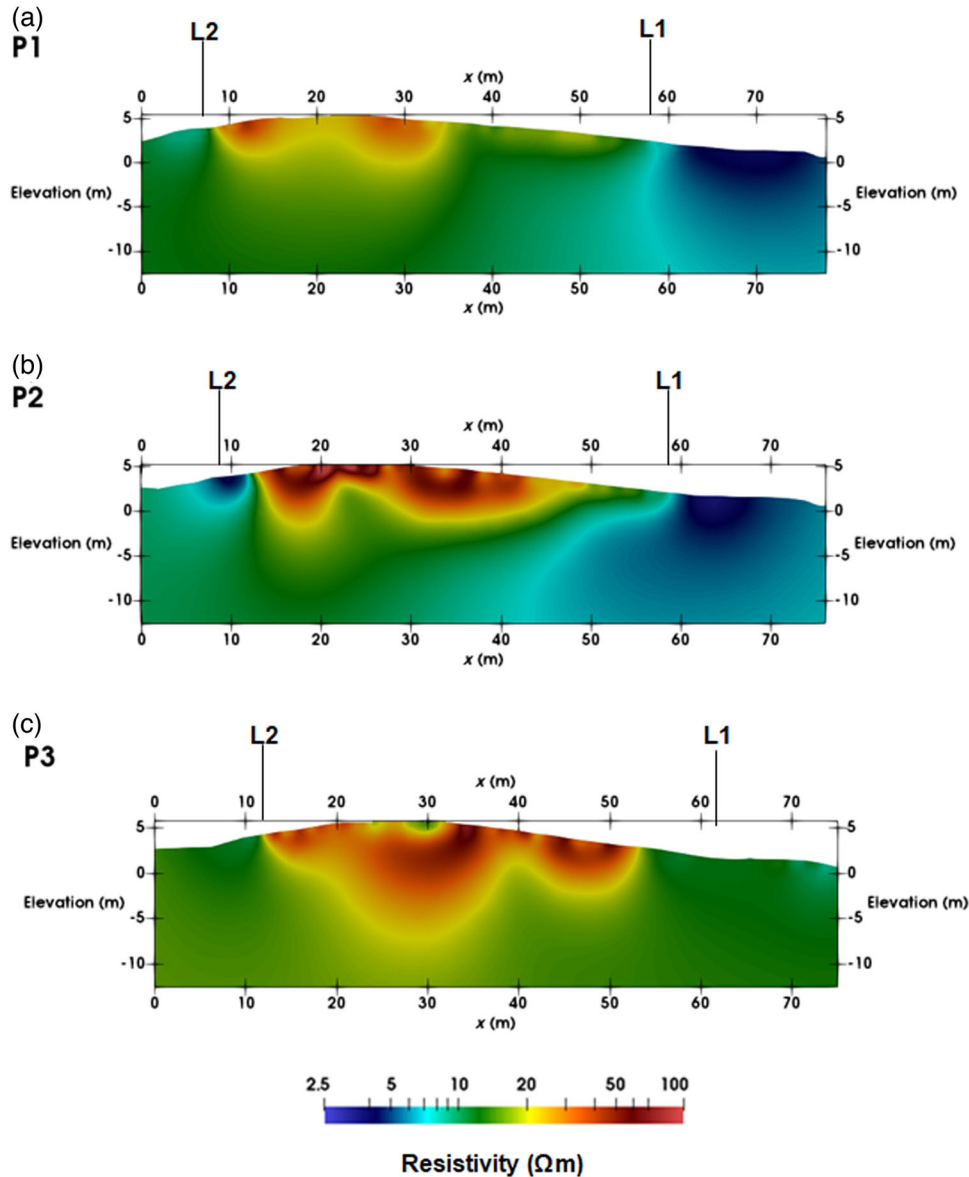
FIGURE 9 2D inversions of lines P1–P3 on 08-Dec-19. (a) Line P1. (b) Line P2. (c) Line P3.

watercourse located adjacent to L1. The region of lower resistivity at depth in L2, observed in the 2D inversions in Figure 7, is not present in the 3D inversion. This implies that it might be a 3D effect that is resolved in a 3D inversion. Through incorporation of the more resistive P1–P3 and L1, the result is a more representative inversion. The general consistency between resistivities through lines indicates that the 3D inversion is able to provide a more reliable representation of the subsurface without influence of a 3D effect. However, the regions in the 3D model between lines P1-P3 are associated with low levels of resolution due to the large line spacings and are therefore not displayed in Figures 11 (and Figure 12, discussed below). Correlation of resistivities within the inversion, mitigating against such 3D effects, is believed to occur where the orthogonal lines cross (i.e. at the intersection between L2 and P1).

To further identify potential changes with a tidal cycle, the results of a 3D difference inversion are shown in Figure 12. The results reveal a distinct change in resistivity at shallow depths. In the 2D inversions and synthetic modelling, it was noted that artefacts induced by the 3D effect were present at depth. The 3D inversions do not show a significant change in resistivity at equivalent depths. Therefore, with a similar resistivity distribution to 2D time-lapse inversions and reduced artefacts in lines proximal to the river, it has been suggested that the 3D inversions are able to successfully visualize subsurface conditions with some mitigation of the 3D effect.
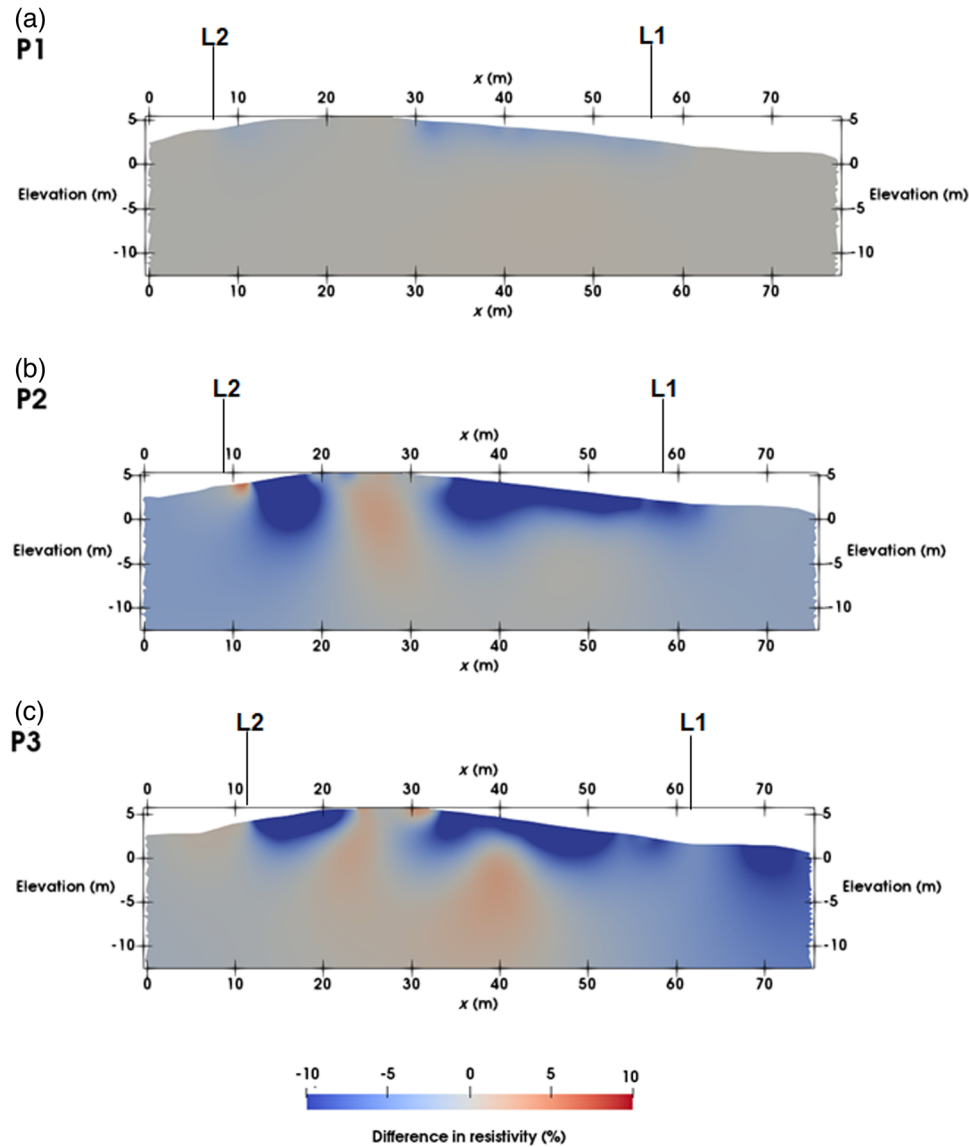
FIGURE 10 2D difference inversions of lines P1–P3 on 08-Dec-19. (a) Line P1. (b) Line P2. (c) Line P3.
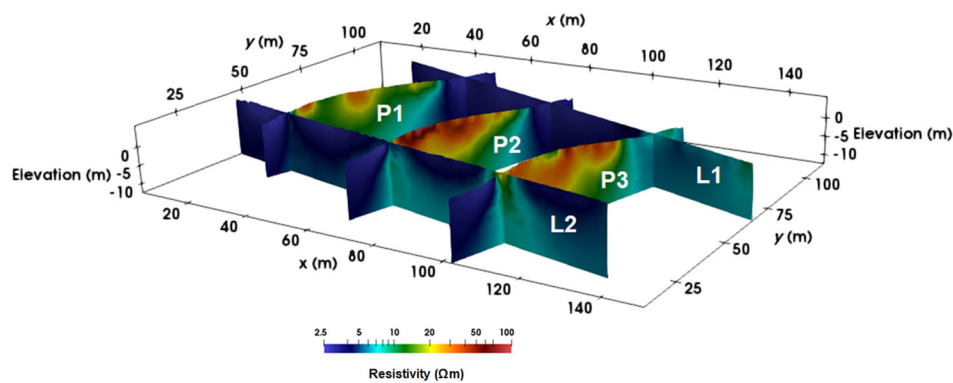

FIGURE 11 3D reference inversion for Hadleigh Marsh, taken from the beginning of the tidal cycle (08-Dec-19), where the maximum tidal ingress is lowest. L2 is adjacent to the River Thames.
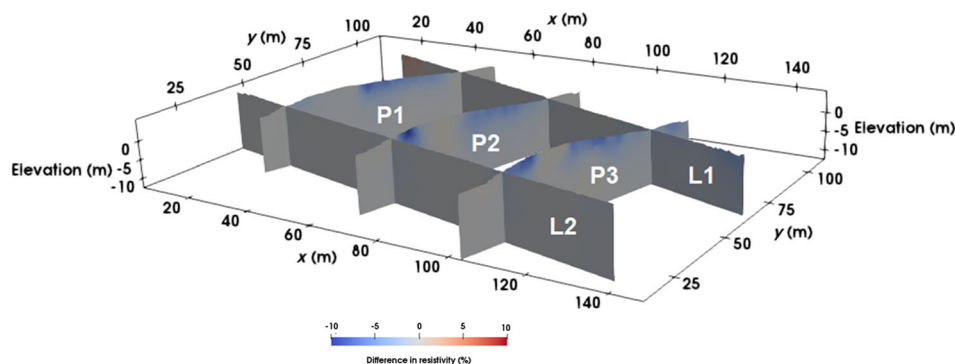
17-Dec-19

FIGURE 12 A 3D time-lapse inversion for Hadleigh Marsh (17-Dec-19), using Figure 11 as a reference, taken from a time period where the maximum tidal height was at its peak. L2 is adjacent to the River Thames.

DISCUSSION

The synthetic modelling explored the effects of changing river salinity and river level upon resistivities beneath the array. For a scenario of a clay embankment with a homogeneous resistivity of 40 Ωm, it has been determined (for the given geometry) that there are unlikely to be any noticeable effects when the river is 4.5 m away from the electrode array and 0.75 m below crest height (for the geometry of this particular model). Within this limit, resistivity will be decreased at greater depths than 2 m underneath the electrode array where electrode spacings are 2 m or less. The nature of the homogeneous embankment is highly idealized, as it is unlikely that a real embankment will be homogeneous, and the trend and magnitude of affected resistivities are highly impacted by the given parameters. For instance, if the embankment resistivity is higher, higher resistivities from the modelled river would likely induce an effect and the resistivities modelled in this case study could create a greater resistivity contrast. Consequently, the trend of resistivity at depth could be more severe and noticeable at river levels deeper and further away from the electrode array than in this synthetic model. In a more coastal environment embankment, resistivities will likely be smaller than that of the synthetic model (40 Ωm). However, modelling a larger embankment resistivity enables more universal applicability, such as for tidally influenced rivers, where river salinity will be low, and to enable comparison between freshwater and saltwater settings.

Different slope angles would enable the possibility of the river to decline further vertically for the lateral movement of the river away from the electrode array. Therefore, with steeper slope angles there could be a more pronounced 3D effect possible, given the river is still proximal, laterally, to the electrode array with increased declines vertically and may be within an influence zone. For embankments with larger heights and wider bases, larger electrode spacings may be chosen for greater depths of investigation. Therefore, embankment geometry is needed to be understood to assess the characteristics of a 3D effect, where different crest heights, base widths and slope angles may impact survey design, the extent of a 3D effect and its magnitude.

The second modelling scenario, with a clay core incorporated into the embankment, provided an opportunity to assess the effect of heterogeneity within the embankment on the 3D effect in the ERT inversions. As with the homogeneous embankment, there was a distinct increase of resistivity at depth with higher river levels, closer to the electrode array. Therefore, the increased heterogeneity modelled within the embankment does not obscure the 3D effect associated with the river at shallow depths. However, embankment heterogeneity influences the inverted model at greater depths, resulting in modelled resistivities from deviating from the true values.

Resistivities of the river have a large influence on the magnitude of the 3D effect. For less resistive river waters, such as brackish conditions typically associated with estuaries, there is likely to be a pronounced 3D effect. Whereas, the higher freshwater resistivities induced negligible 3D effects on the synthetic ERT survey. This highlights the greater need to be aware of potential 3D effects, particularly in estuarine environments, and a need to account for such when working with data obtained from these environments. Freshwater river fluctuations are less likely to induce a 3D effect in environments similar to the synthetic model. However, natural embankments will be more complex, comprising a greater range of resistivities, where elevated water saturation will likely decrease resistivities in the embankment close to the river. This is more difficult to model for generation of 3D effects in a generalized manner or to differentiate the influence of the two contributing

factors (river water level change and changes in soil water content). A heterogeneous model was developed, but no single synthetic modelling scenario is likely to represent a real embankment.

Real resistivities of an embankment will vary over a scale of centimetres and the composition may be highly varied and form irregular layers. The range of resistivities for typical embankment infill, including clay infill, can be higher or lower than what was modelled (Palacky, 1987), so with more resistive infill freshwater may induce a 3D effect with larger ranges in values.

River geometries for the synthetic model have been assumed to be close to the crest height at its peak. Many rivers will be at lower depths and further lateral distances to the electrode array in many survey settings, which could mean they are beyond any influence zone to the ERT data. As such, this shows that for many cases it will be unlikely that large artefacts will be induced in the ERT data, arising from river level fluctuations, and that this study represents a more extreme scenario (e.g., rising water level after a storm event). However, the highly variable nature of a real-life setting to the synthetic model means that there may be some contexts where a 3D effect is likely, due to a strong resistivity contrast between embankment infill and river or highly saline water. Therefore, it is suggested that river levels with the tide and anticipated resistivities of the river and local geology are known for the survey, in order to enable an estimation of whether a 3D effect is likely.

Electrode spacings of 1, 2 and 4 m were modelled in our synthetic study. It was noted that there is a steep decrease in shallow resistivity with increased electrode spacing, due to the lower resolution at shallower depths, resulting in a greater influence zone for the river to impact data. A larger depth of penetration with increased electrode spacing will enable a 3D effect to be reliably detected at greater depths below the electrode array. Resistivities resulting from 1 m or 2 m spacing give similar values, but electrode of spacings 4 m give marked distortions in resistivity, including at shallow depth. This suggests that when shallow resolution is poorer, there is greater influence from the river as a 3D effect when there are fewer resistivity values at shallow depths beneath the ERT array. All electrode spacings show some distortion at resistivity at greater depth.

The analysis of inversions at Hadleigh Marsh indicates the potential for a 3D effect to influence data and potentially mislead interpretation through artefacts being introduced to the data. The most notable is a feature of abnormally low resistivity located at 2 m depth in survey line L2 when inverted in 2D. This corresponds to observed regions of lower resistivity in the synthetic modelling study, caused by the river. With increased maximum tide height during the month, as observed in the time-lapse inversions, there is a decreased resistivity at depth in the area of L2 closest to the river. This

suggests that the anomalous region of lower resistivity in L2 is probably a 3D effect resulting from the river, which could incorrectly be interpreted to be a region of saline water beneath the array instead. At high tide, resistivities are over 5% less resistive at depth than at low tide. Therefore, sites with pronounced tidal ranges will experience greater potential 3D effects, and sites which are more resistive will see greater resistivity contrasts between artefacts induced by a 3D effect and the embankment resistivity, potentially leading to a greater degree of misinterpretation. When data are inverted in 3D, there is no noticeable conductive region at depth in L2, indicating that 3D inversions could rectify the observed 3D effect in L2 and that incorporating a 3D inversion scheme could aid interpretation of ERT data in tidal settings.

Previous research on an off-centre pipeline had inferred that electrode spacing is unlikely to alter 3D effect magnitudes (Hung et al., 2019), whereas laboratory experimentation and synthetic modelling of different electrode spacings with a change in water infiltration had suggested that increased electrode spacings would increase the 3D effect until shallow resolution had decreased substantially (Hojat et al., 2020). The synthetic modelling here indicates with increased electrode spacing there is more severe decrease in resistivity from a 3D effect, supporting that electrode spacing does alter 3D effect magnitudes. It is therefore suggested that where the suspected source of a 3D effect is larger than the survey, electrode spacings are kept to a minimum feasible level for survey requirements to reduce a 3D effect on surveying at shallow depths if the survey is to be inverted in 2D.

To account for such issues when they are expected, it is suggested that 3D ERT inversions are undertaken where the survey locations are proximal to a river. 3D inversions can incorporate the full embankment geometry and also the resistivity of the adjacent water course. A 3D inversion would reduce the potential artefacts resulting from a 3D effect linked to the river, as observed at Hadleigh Marsh. Ideally, this would involve a 3D ERT survey geometry, which would allow greater restriction of resistivities across the embankment area. However, time and geometrical constraints may prevent a true 3D ERT survey. Utilization of a 3D inversion scheme across all lines at Hadleigh Marsh reduced the 3D effect, suggesting that this suppressed 3D effects from 2D inversion, and previous research indicates that incorporating 3D coverage of potential measurements suppresses the 3D effect (Sjödahl et al., 2006). Whereas, with a singular ERT line in the synthetic model the 3D effect is noticeable. Therefore, to constrain 3D effects, the survey should ideally incorporate more than one line in a series of arrays which cross-cut each other across the survey region and can then be inverted using a 3D approach.

If designing a time-lapse ERT set-up, it is recommended that a reconnaissance survey is undertaken for design of the time-lapse system, where several surveys are run during the day at different times, and with more than one survey line, to account for the effect of distance from the river. This will enable interpretation of how any 3D effect present varies with tide across the day and survey distance from the river, for optimal survey design for later time-lapse monitoring. From the interpretation of the reconnaissance survey, electrode arrays can be located outside of areas with suspected 3D effects present and survey times set for when the tide is forecast to be low, although this will clearly limit to potential to monitor the integrity of the barrier under such events. For surveys close to a river that could create 3D effects, survey design should ideally include several arrays, which are proximal to each other and provide orthogonal coverage of the area. Such surveys, coupled with recognition of the river feature in any forward modelling, will allow fully 3D inversions to be carried out, eliminating 3D effects due to the watercourse.

Future research involving mathematically determining the extent of likely influence for a range of given parameters (e.g., embankment infill resistivity, number of layers, river resistivity) could enable specification for survey design, giving boundaries for survey design as to where 3D surveying may be necessary to mitigate potential 3D effects. Investigation of more complex embankment geometries could be developed to account for 3D effects in other embankment settings. Also, normalization techniques could be developed to reduce the influence of a proximal river, as Fargier et al. (2014) and Bièvre et al. (2018) have utilized for reducing topographic-induced artefacts.

CONCLUSIONS

A synthetic modelling exercise was developed to assess the change in 3D effect associated with changing river levels, salinities and electrode spacings for a homogeneous and heterogeneous embankment. From this, it was seen that there is a clear 3D effect induced with river resistivities associated with more brackish water, indicating that estuaries are likely to induce a 3D effect on proximal surveys. The 3D effect is noticeable at river distances less than 4.5 m in lateral distance and 0.75 m in vertical height from the electrode array and embankment crest height, respectively. Therefore, a significant 3D effect is most likely where ERT surveys are taken on the riverside flank of an embankment and are unlikely to be impacted where surveys are taken on the landward side. Though specific boundaries for where a 3D effect from a tidal river may be influential are controlled by embankment geometry, the local geology and water content and it is suggested that local conditions are considered for each survey, since the 3D effect may have a greater or smaller influence distance for different scenarios.

Using time-lapse inversion data taken from tidal cycles at Hadleigh Marsh and modelling of a synthetic embankment, the impacts of the 3D effect have been identified and evaluated, where the nature of the synthetic model has guided interpretation of the presence of the 3D effect at the site and given assessment to whether a 3D effect from tidal action is likely to be experienced in ERT surveys. At Hadleigh Marsh, there was an associated resistive low in data adjacent to the Thames, at depths equivalent to observed 3D effects in the synthetic modelling and areas most proximal to the river, indicating that there is a likelihood that a 3D effect is impacting the data. With greater resistivities, such effects will be more distinguishable and the anomalous resistivities may lead to misinterpretation. This shows a need to address 3D effects resulting from estuaries, which has been explored further in synthetic modelling to assess likely extents of a 3D effect in this environment.

Electrode spacings of 2 m or less in survey sequences have been suggested (for the geometry studied here) to minimize the potential influence from the river on the ERT survey at shallow depths. Alongside this, we recommend that 3D ERT surveying is set up on the riverside of an embankment to reduce artefacts from the water body with a greater degree of resolution in the inversion. If this is not possible, it is suggested that several linear ERT arrays are used (e.g. parallel and/or orthogonal survey lines), which can be inverted using a 3D scheme to reduce potential 3D effects. This study highlights the potential for a 3D effect to be induced in estuarine environments, due to the likely saline water and potential high resistivity contrasts. Future work in this field will involve modelling of more complex embankment geologies and means of reducing any effect

DATA AVAILABILITY STATEMENT
The data which supports the research can be made available upon request of the author.

ORCID

John Ball ⓘ https://orcid.org/0000-0002-8350-7266

Jonathan Chambers ⓘ https://orcid.org/0000-0001-6215-6535

Paul Wilkinson ⓘ https://orcid.org/0000-0002-8135-776X

Andrew Binley ⓘ https://orcid.org/0000-0002-0938-9070

REFERENCES

Almog, E., Kelham, P. & King, R. (2011) *Modes of dam failure and monitoring and measuring techniques*. Bristol, UK: Environment Agency.

Amabile, A., de Carvalho Faria Lima Lopes, B., Pozzato, A., Benes, V. & Tarantino, A. (2020) An assessment of ERT as a method to monitor water content regime in flood embankments: The case study of the Adige River embankment. *Physics and Chemistry of the Earth*, 120, 102930. https://doi.org/10.1016/j.pce.2020.102930

Bersan, S., Koelewijn, A. & Simonini, P. (2018) Effectiveness of distributed temperature measurements for early detection of piping in river embankments. *Hydrology and Earth System Sciences*, 22(2), 1491–1508. https://doi.org/10.5194/hess-22-1491-2018

Bièvre, G., Oxarango, L., Günther, T., Goutaland, D. & Massardi, M. (2018) Improvement of 2D ERT measurements conducted along a small earth-filled dyke using 3D topographic data and 3D computation of geometric factors. *Journal of Applied Geophysics*, 153, 100–112. https://doi.org/10.1016/j.jappgeo.2018.04.012

Binley, A. & Slater, L. (2020) *Resistivity and Induced Polarization: Theory and Applications to the Near-Surface Earth*. Cambridge, UK: Cambridge University Press. https://doi.org/10.1017/9781108685955

Blanchy, G., Saneiyan, S., Boyd, J., McLachlan, P. & Binley, A. (2020) ResIPy, an intuitive open source software for complex geoelectrical inversion/modeling. *Computers and Geosciences*, 137, 104423. https://doi.org/10.1016/j.cageo.2020.104423

Borgatti, L., Forte, E., Mocnik, A., Zambrini, R., Cervi, F., Martinucci, D. et al. (2017) Detection and characterization of animal burrows within river embankments by means of coupled remote sensing and geophysical techniques: lessons from River Panaro (northern Italy). *Engineering Geology*, 226, 277–289. https://doi.org/10.1016/j.enggeo.2017.06.017

Brand, J.H. & Spencer, K.L. (2019) Potential contamination of the coastal zone by eroding historic landfills. *Marine Pollution Bulletin*, 146, 282–291. https://doi.org/10.1016/j.marpolbul.2019.06.017

Camarero, P.L., Moreira, C.A. & Pereira, H.G. (2019) Analysis of the Physical Integrity of Earth Dams from Electrical Resistivity Tomography (ERT) in Brazil. *Pure and Applied Geophysics*, 176(12), 5363–5375. https://doi.org/10.1007/s00024-019-02271-8

Cardarelli, E., Cercato, M. & De Donno, G. (2014) Characterization of an earth-filled dam through the combined use of electrical resistivity tomography, P- and SH-wave seismic tomography and surface wave data. *Journal of Applied Geophysics*, 106, 87–95. https://doi.org/10.1016/j.jappgeo.2014.04.007

Chambers, J.E., Gunn, D.A., Wilkinson, P.B., Meldrum, P.I., Haslam, E., Holyoake, S. et al. (2014) 4D electrical resistivity tomography monitoring of soil moisture dynamics in an operational railway embankment. *Near Surface Geophysics*, 12(1), 61–72. https://doi.org/10.3997/1873-0604.2013002

Cho, I.K., Ha, I.S., Kim, K.S., Ahn, H.Y., Lee, S. & Kang, H.J. (2014) 3D effects on 2D resistivity monitoring in earth-fill dams. *Near Surface Geophysics*, 12(1), 73–81. https://doi.org/10.3997/1873-0604.2013065

Dunbar, J.B., Galan-comas, G., Walshire, L.A., Wahl, R.E., Yule, D.E., Corcoran, M.K. et al. (2017) Remote sensing and monitoring of earthen flood-control structures. Geotechnical and Structures Laboratory (Issue July). pp. 1–307.

Environment Agency. (2017) *Flood map for planning (rivers and sea) GIS dataset*. Bristol, UK: Environment Agency.

Essex County Council. (n.d.) *Landfill Site Information Sheet, Site Name*: Hadleigh Sea Wall. Essex County Council.

Fargier, Y., Lopes, S.P., Fauchard, C., François, D. & Côte, P. (2014) DC-electrical resistivity imaging for embankment dike investigation: A 3D extended normalisation approach. *Journal of Applied Geophysics*, 103, 245–256. https://doi.org/10.1016/j.jappgeo.2014.02.007

Geuzaine, C. & Remacle, J. (2020) Gmsh: A three-dimensional finite element mesh generator with built-in pre- and post-processing facilities. https://gmsh.info/

Gunn, D.A., Chambers, J.E., Dashwood, B.E., Lacinska, A., Dijkstra, T., Uhlemann, S. et al. (2018) Deterioration model and condition monitoring of aged railway embankment using non-invasive geophysics. *Construction and Building Materials*, 170, 668–678. https://doi.org/10.1016/j.conbuildmat.2018.03.066

Hojat, A., Arosio, D., Ivanov, V.I., Loke, M.H., Longoni, L., Papini, M. et al. (2020) Quantifying seasonal 3D effects for a permanent electrical resistivity tomography monitoring system along the embankment of an irrigation canal. *Near Surface Geophysics*, 18(4), 427–443. https://doi.org/10.1002/nsg.12110

Holmes, J., Chambers, J., Meldrum, P., Wilkinson, P., Boyd, J., Williamson, P. et al. (2020) Four-dimensional electrical resistivity tomography for continuous, near-real-time monitoring of a landslide affecting transport infrastructure in British Columbia, Canada. *Near Surface Geophysics*, 18(4), 337–351. https://doi.org/10.1002/nsg.12102

Hung, Y.C., Lin, C.P., Lee, C.T. & Weng, K.W. (2019) 3D and boundary effects on 2D electrical resistivity tomography. *Applied Sciences (Switzerland)*, 9(15), 2963. https://doi.org/10.3390/app9152963

Jodry, C., Palma Lopes, S., Fargier, Y., Sanchez, M. & Côte, P. (2019) 2D-ERT monitoring of soil moisture seasonal behaviour in a river levee: a case study. *Journal of Applied Geophysics*, 167, 140–151. https://doi.org/10.1016/j.jappgeo.2019.05.008

Jones, G., Sentenac, P. & Zielinski, M. (2014) Desiccation cracking detection using 2-D and 3-D electrical resistivity tomography: validation on a flood embankment. *Journal of Applied Geophysics*, 106, 196–211. https://doi.org/10.1016/j.jappgeo.2014.04.018

LaBrecque, D.J. & Yang, X. (2001) Difference inversion of ERT data: a fast inversion method for 3-D in situ monitoring. *Journal of Environmental and Engineering Geophysics*, 6(2), 83–89.

Michalis, P, Sentenac, P. & Macbrayne, D. (2016) Geophysical assessment of dam infrastructure: the Mugdock Reservoir Dam case study. In the Third Joint International Symposium on Deformation Monitoring, 30 March–1 April 2016, Vienna, Austria, pp. 1–6.

Michalis, P. & Sentenac, P. (2021) Subsurface condition assessment of critical dam infrastructure with non-invasive geophysical sensing. *Environmental Earth Sciences*, 80(17), 556. https://doi.org/10.1007/s12665-021-09841-x

Moore, J.R., Boleve, A., Sanders, J.W. & Glaser, S.D. (2011) Self-potential investigation of moraine dam seepage. *Journal of Applied Geophysics*, 74(4), 277–286. https://doi.org/10.1016/j.jappgeo.2011.06.014

Nimmer, R.E., Osiensky, J.L., Binley, A.M. & Williams, B.C. (2008) Three-dimensional effects causing artifacts in two-dimensional, cross-borehole, electrical imaging. *Journal of Hydrology*, 359(1–2), 59–70. https://doi.org/10.1016/j.jhydrol.2008.06.022

Palacky, G. (1987) Resistivity characteristics of geological targets. In *Electromagnetic Methods in Applied Geophysics-Theory*. Houston, TX: Society of Exploration Geophysicists, pp. 53–129.

Planès, T., Mooney, M.A., Rittgers, J.B.R., Parekh, M.L., Behm, M. & Snieder, R. (2016) Time-lapse monitoring of internal erosion in earthen dams and levees using ambient seismic noise. *Géotechnique*, 66(4), 301–312. https://doi.org/10.1680/jgeot.14.P.268

Rittgers, J.B., Revil, A., Planes, T., Mooney, M.A. & Koelewijn, A.R. (2015) 4-D imaging of seepage in earthen embankments with

time-lapse inversion of self-potential data constrained by acoustic emissions localization. *Geophysical Journal International*, 200(2), 756–770. https://doi.org/10.1093/gji/ggu432

Sandrin, T.R., Dowd, S.E., Herman, D.C. & Maier, R.M. (2009) Aquatic environments. In: Maier, R.M., Pepper, I.L. & Gerba, C.P. (Eds.) *Environmental microbiology*, 2nd edition. Amsterdam: Academic Press Elsevier, pp. 103–122. https://doi.org/10.1016/B978-0-12-370519-8.00006-7

Secretary of State. (2002) *The Landfill (England and Wales) Regulations 2002*. Environmental Protection, England and Wales.

Sentenac, P., Benes, V. & Keenan, H. (2018) Reservoir assessment using non-invasive geophysical techniques. *Environmental Earth Sciences*, 77(7), 1–14. https://doi.org/10.1007/s12665-018-7463-x

Sjödahl, P., Dahlin, T. & Zhou, B. (2006) 2.5D resistivity modeling of embankment dams to assess influence from geometry and material properties. *Geophysics*, 71(3), G107. https://doi.org/10.1190/1.2198217

Tresoldi, G., Hojat, A. & Zanzi, L. (2018) Correcting the influence of 3D geometry to process 2D ERT monitoring data of river embankments at the laboratory scale. In: *37 Convegno GNGTS 2018*, Bologna, Italy: GNGTS. pp. 690–694

Tresoldi, G., Arosio, D., Hojat, A., Longoni, L., Papini, M. & Zanzi, L. (2019) Long-term hydrogeophysical monitoring of the internal conditions of river levees. *Engineering Geology*, 259(August 2018), 105139. https://doi.org/10.1016/j.enggeo.2019.05.016

Wang, F., Okeke, A.C.U., Kogure, T., Sakai, T. & Hayashi, H. (2018) Assessing the internal structure of landslide dams subject to possible piping erosion by means of microtremor chain array and self-potential surveys. *Engineering Geology*, 234, 11–26. https://doi.org/10.1016/j.enggeo.2017.12.023

Yang, K.H. & Wang, J.Y. (2018) Closure to discussion of "experiment and statistical assessment on piping failures in soils with different gradations. *Marine Georesources and Geotechnology*, 36(3), 376–378. https://doi.org/10.1080/1064119X.2017.1321072

Zhang, J. & Revil, A. (2015) 2D joint inversion of geophysical data using petrophysical clustering and facies deformation. *Geophysics*, 80(5), M69–M88. https://doi.org/10.1190/geo2015-0147.1